TECHNICAL TRANSACTIONS | **CZASOPISMO TECHNICZNE**
ELECTRICAL ENGINEERING | ELEKTROTECHNIKA

3-E/2016

DOI: 10.4467/2353737XCT.16.269.6068

JAROSŁAW TULICKI, JANUSZ PETRYNA, MACIEJ SUŁOWICZ*

FAULT DIAGNOSIS OF INDUCTION MOTORS IN SELECTED WORKING CONDITIONS BASED ON AXIAL FLUX SIGNALS

DIAGNOSTYKA SILNIKA INDUKCYJNEGO W WYBRANYCH STANACH PRACY NA PODSTAWIE SYGNAŁU STRUMIENIA POOSIOWEGO

Abstract

The article presents the possibility of using axial flux signals in the fault diagnosis of low-power induction machines working under varying load conditions. The study involved cases of asymmetrical rotors and stators in steady state and transient conditions during start-up. The laboratory measurements were performed on a modified induction motor, which was equipped with a special coil built into the bearing shield allowing the measurement of the voltage proportional to the motor axial flux. Examples of the obtained waveforms and numerical data were supplemented by conclusions and a review of current knowledge concerning the application of the axial flux signal for the purpose of the fault diagnosis of squirrel cage induction motors.

Keywords: asymmetry induction motor, axial flux, diagnostics

Streszczenie

Artykuł przedstawia możliwość zastosowania sygnału strumienia poosiowego w diagnostyce maszyn indukcyjnych małej mocy, pracujących przy zmiennych warunkach obciążenia. Badaniom poddano przypadki niesymetrii wirnika i obwodu stojana dla stanu ustalonego oraz przejściowego. Pomiary laboratoryjne zostały wykonane na zmodyfikowanym silniku, przystosowanym do pomiaru napięcia wprost proporcjonalnego do strumienia unipolarnego, za pomocą wbudowanej cewki w tarczy łożyskowej. Przykłady uzyskanych przebiegów oraz danych liczbowych uzupełniono o wnioski i przegląd dotychczasowej wiedzy z zakresu zastosowania sygnału strumienia poosiowego w diagnostyce maszyn klatkowych.

Słowa kluczowe: asymetria silnika indukcyjnego, strumień osiowy, diagnostyka

* M.Sc. Eng. Jarosław Tulicki, Ph.D. Eng. Janusz Petryna, Ph.D. Eng. Maciej Sułowicz, Department of Electrical and Computer Engineering, Institute of Electromechanical Conversion, Cracow University of Technology.

1. Introduction

The basic diagnostic signals in the induction motor are the voltage and current signals of the stator circuit. In addition to the values of the currents in the windings of the stator and the rotor, the level of the magnetic flux is another distinctive feature of induction motors. In symmetrical induction machines, flux linkages have a component only in a radial direction. For any asymmetry of induction motors, flux linkages decompose themselves additionally into an axial component. The axial component causes not only additional losses in the stator end-windings, but it also acts as a carrier of diagnostic information contained in the electromagnetic field time harmonics available by the measurement [1, 6, 7]. As it was proved in articles [2, 9, 10, 11, 13, 14, 19], an analysis of the axial flux course allows an effective identification of damage to the stator circuit in the form of coil turn short- circuits and rotor asymmetry. The article presents selected results of the authors' research on the application of the axial flux in the fault diagnosis of low-power induction motors [17, 18]. In the article, a comparison to the stator current analysis was made under similar conditions to those under which the axial flux waveforms were analysed.

1.1. Method of measurement of the axial flux

The main element used for detecting changes of the axial flux in time is the coreless coil. The coil acts as a secondary winding in which a voltage, whose actual value is the time derivative of flux, is induced by the action of the alternating axial flux.

As it can be seen, the main metrological feature of the air coil is lack of nonlinear distortions and its characteristic similar to that of a band-pass filter.

a)

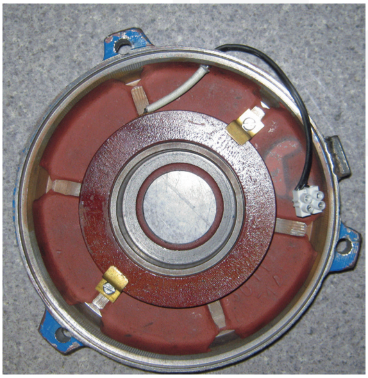

b)

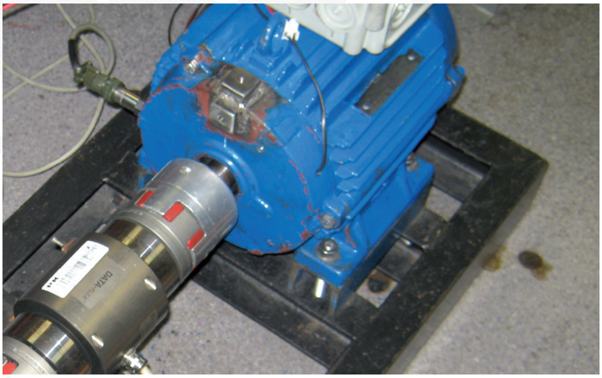

Fig. 1. View of measuring coil: a) inside the bearing shield, b) mounted inside the motor housing

In terms of mechanical structure, the diameter of the carcass is a very important parameter. The diameter of the carcass cannot be either less than the diameter of the rotor or greater than the diameter of the stator [7, 10]. Typically, the measuring coil is mounted on the fan cover or inside the bearing shield [6] – it is rarely mounted on the motor body [3]. Fig. 1 shows a view of the measuring coil used in the laboratory and its assembly inside the motor housing.

2. Measuring system

The subject of the study was the induction motor type Sg-112M-4. The motor was mechanically connected to a separately-excited DC generator by means of the Rotex flexible claw coupling and the DataFlex 22/50 measuring shaft with integrated measuring speed system. The DC generator provided a mechanical load to the induction motor.

The load torque was adjusted by changing the generator excitation current – an autotransformer with a rectifier was used for this purpose. The DC generator output was loaded by 4 kW set of resistive heating elements. The NI USB 6259 multifunctional measuring card was used for the acquisition of measurement signals. The duration of data recording for a single measurement was 10 seconds – the signals were recorded with a sampling frequency of 10 kS/s per channel. In addition to measuring the coil voltage and the shaft speed and torque, the phase voltage and current waveforms were recorded with the use of the transducers LEM LV 25-P and HY15-P.

a) b)

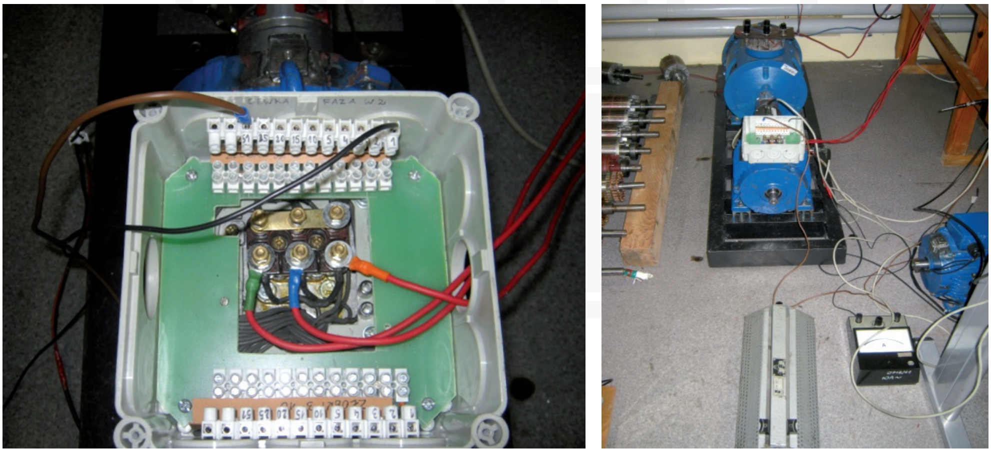

Fig. 2. Laboratory view of: a) modified terminal box, b) induction motor with measuring instruments

Several simulated damages to the rotor were realized by the use of rotors with different degrees of asymmetry. In the research, a symmetrical rotor and other two damaged rotors: one with one broken bar and the other one with two broken bars, were used.

For the purposes of the research, some modifications to the stator windings and the terminal box were required. The stator winding modification allowed the short-circuiting of a selected number of turns in phase ‘W’ by the use of the 6–40 Ω control resistor and an ammeter to limit the short-circuit current. During the measurements, the induction motor phases were connected in the star configuration. The motor was supplied from the rigid network and operated without its cooling fan. The fan was removed because of the possible generation of additional rotary components in the frequency spectrum related directly to the number of fan blades. Before the measurements session, the drive system was aligned. All calculations and measurements were performed using the Matlab software. Fig. 2 shows views of the laboratory stand together with the measuring instruments.

3. Diagnostic signals

3.1. Asymmetry of the rotor cage

In the case of rotor asymmetry (as damaged bars or dynamic eccentricity), the spectrum of the voltage proportional to the axial flux contains noticeable components described by the following equation [6, 7]:

$$f_r = f_0\ [s + k(1 - s)] \tag{1}$$

where:

f_r – frequency associated with the asymmetrical rotor;
f_0 – fundamental frequency;
s – slip;
k – 3, 5, 7… .

Additionally, regardless of the rotor condition, from among the spectrum components, besides the mains frequency and its odd multiples, the first slip component can be identified [6, 11] as:

$$f_{s1} = f_0 s \tag{2}$$

where:

f_{s1} – primary slip frequency.

Based on equation (2) and design parameters of an induction motor as demonstrated in [9, 19], it is possible to reproduce courses of the torque and rotor speed in time domain.

Among additional frequencies related to the rotor asymmetry described by equation (1), in the spectrum of the measuring coil voltage, the following components described by equation (3) can be observed:

$$f_{sw} = k f_0\ s \tag{3}$$

where:

f_{sw} – another successive odd slip frequency.

Also in the case of analysis of the axial flux signal, the diagnostic signal (commonly used to analyse the stator current and to detect rotor cage asymmetry and dynamic eccentricity [6, 7, 15, 19]) described by the equation (4), was applied:

$$f_b = f_0\ (1 - 2s) \tag{4}$$

where:

f_b – left sideband slip frequency.

It should be noted that on the basis of equations (3) and (4), a damage to the joint rings of the rotor cage can be detected. However, in the case of the stator current analysis, the distinction between the damage to the rotor bars and to the joint rings is not possible in practice [6, 15].

3.2. Asymmetry of the stator

A common cause of asymmetry of the stator circuit are inter-turn short-circuits inside a single phase of the winding or inter-phase short-circuits leading to the rapid failure of the induction motor [3, 6]. As indicated in the introduction, the analysis of voltage proportional to the axial flux allows the detection of inter-turn short-circuits already in the initial stage of damage. The main diagnostic signal in the form of spectrum components for the short-circuits detection in the stator winding can be described by the following formula [3, 6, 7]:

$$f_k = k f_0 + [n_s(1 - s)\, m]/60 \tag{5}$$

or

$$f_k = k f_0 + n\, m/60 \tag{6}$$

where:

f_k – frequency appearing when short-circuiting;

n_s – synchronous speed;

m – –2, –1, +1, +2, …

n – motor speed.

As it can be seen, the frequencies of the spectrum components depend on design parameters of the induction motor as the number of pole pairs and supply frequency.

4. Measurement results and analysis

4.1 Stationary analysis

Spectral analysis of the steady state signal [4, 15, 16] is one of the basic methods for assessing the condition of a rotor and stator. When attempting to identify the characteristic signs of damage within the spectrum of stator current, it is necessary to provide and maintain the specified measurement conditions. When testing a low- and medium-power induction motor, it should be loaded at least half the nominal torque [15].

Furthermore, the drive system should be free of defects in mechanical connections, such as a misalignment for example, while the rotor unbalance influences the quality of the measurements slightly less. Failure to meet these conditions regarding the tested induction motor leads to disorder in the readability of the current spectrum, making proper separation of diagnostic components impossible. It should also be mentioned that a direct spectral analysis of the stator phase current does not allow to detect the stator asymmetry caused by an insignificant number of shorted turns inside a single stator phase.

The axial flux signal (expressed in an intermediate form of the voltage waveform where influence of load torque values and supply frequency [6, 7] on readability of the spectrum voltage is minimal) is free of the above drawbacks [17, 18]. In addition, as it will be shown later in this article, the axial flux signal shows high sensitivity to any asymmetries of electrical origin. Below, some chosen measurements and the FFT spectrum calculations results for an induction motor with rotor and stator asymmetry are presented. The amplitude spectrum was limited to a band of 200 Hz. The resulting diagrams were produced on a linear scale (Fig. 4–6). Some selected examples were obtained for an induction motor running in the steady state with the stator load current 4.5 amps.

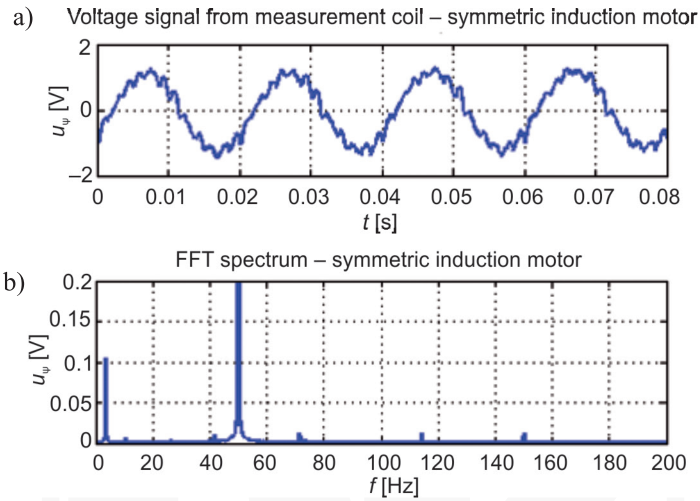

Fig. 3. Symmetrical induction motor: a) voltage signal from measurement coil, b) FFT spectrum

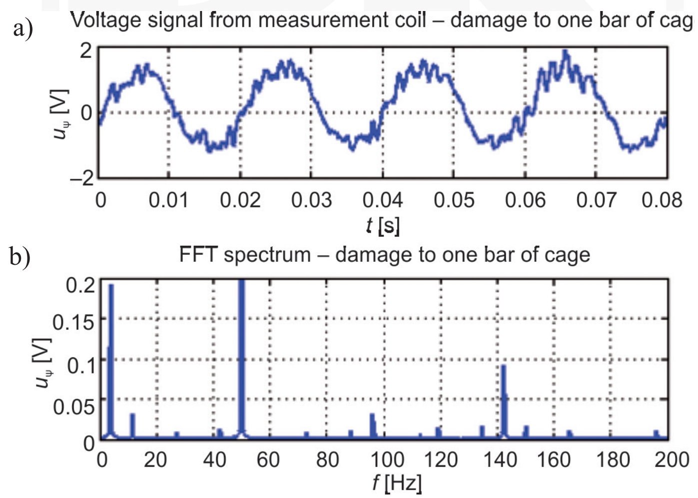

Fig. 4. Damage to one bar of cage: a) voltage signal from measurement coil, b) FFT spectrum

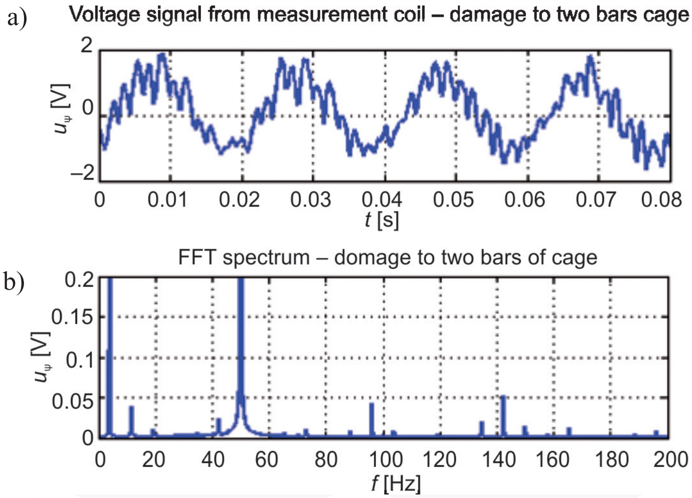

Fig. 5. Damage to two bars of cage: a) voltage signal from measurement coil, b) FFT spectrum

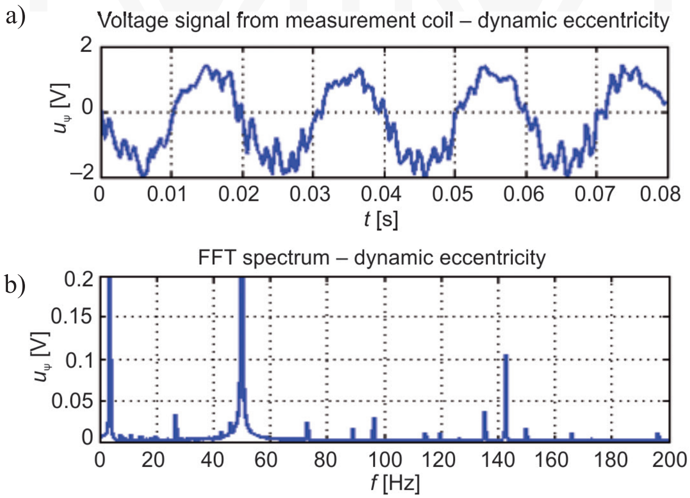

Fig. 6. Dynamic eccentricity 40%: a) voltage signal from measurement coil, b) FFT spectrum

In the case of an induction motor damage resulting in an asymmetry of the rotor cage, it can be shown that the damages to the cage bars cause a significant increase in component amplitudes described by formulas (1) to (4), while at the same time, they cause a decrease of the supply fundamental component amplitude (Tab. 1). For dynamic eccentricity, like in the case of the damages to the bars, the growth of the amplitudes of the components (1) and (4) can be observed, in the absence of changes in the component (3) as compared with a symmetrical induction motor. Based on the conclusions made, it can be stated that the preliminary assessment of dynamic eccentricity is possible on the basis of odd multiple components of slip frequency (3) and seems to be an important supplement to the method based on searching slot harmonics in the band of mid-frequency spectrum [19].

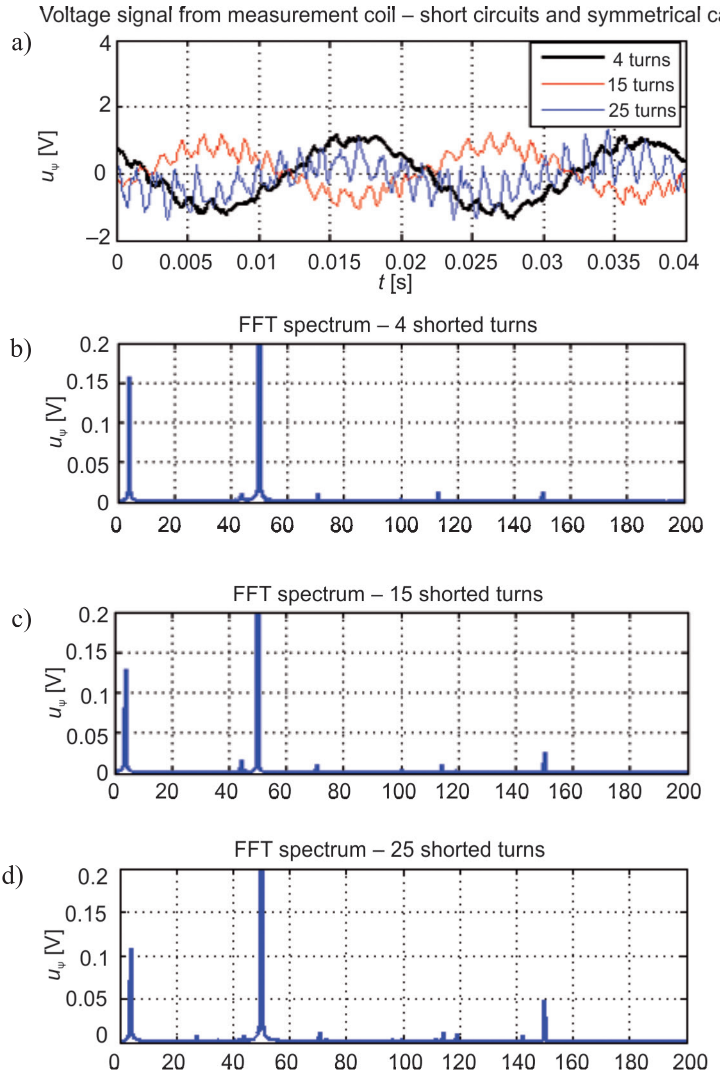

Fig. 7. Short circuits and the symmetrical cage: a) voltage signal from measurement coil, b), c), d) FFT spectrum for different number of shorted turns

a)

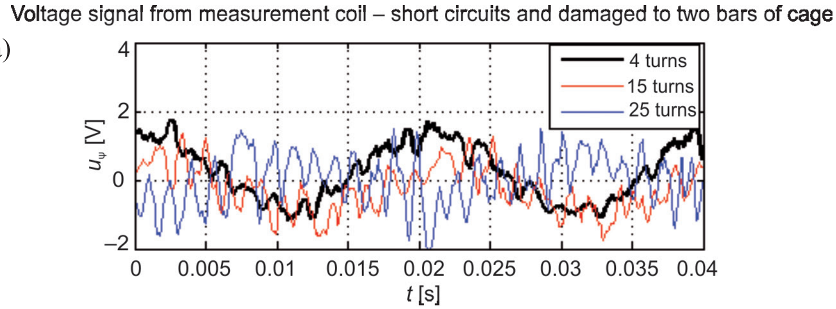

b)

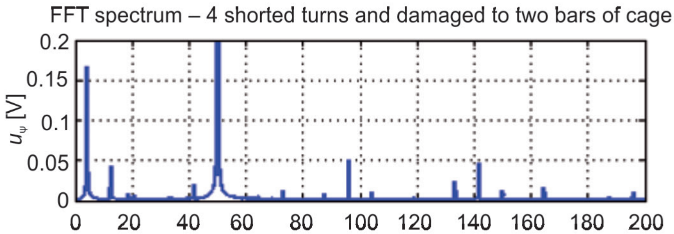

c)

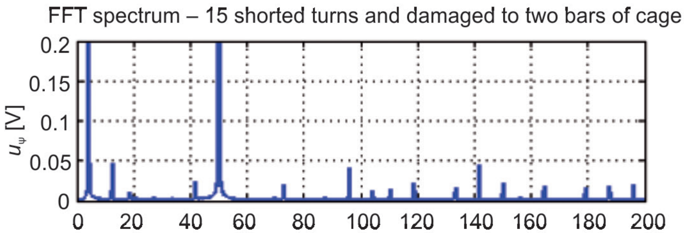

d)

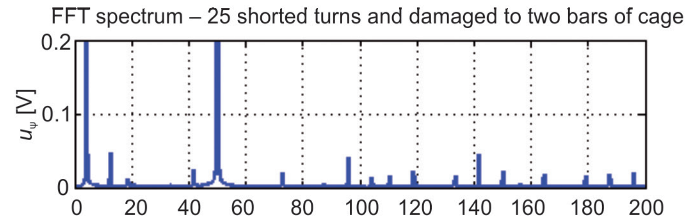

Fig. 8. Short circuits and two bars of cage damaged: a) voltage signal from measurement coil, b), c), d) FFT spectrum – shorted turns and two bars of cage damaged

Table 1

Values of the diagnostic signals from FFT spectrum

Type of damage	Diagnostic signals [V/Hz]						
	$f_0\ s$	$3f_0\ s$	$5f_0\ s$	$f_0\ (1-2s)$	f_0	$3f_0$	$f_0[s+3(1-s)]$
Symmetric motor	0.104/3.5	0.006/10.5	0.00046/24.5	0.0046/43	1.35/ 50	0.14/150	0.0006/143
One bar of cage	0.192/3.8	0.032/11.4	0.002/19.3	0.012/42.4	1.20/ 50	0.15/150	0.092/142.4
Two bars of cage	0.208/3.8	0.04/11.4	0.010/19.3	0.022/42.3	0.94/ 50	0.16/150	0.052/142.3
Dynamic Eccentricity	0.202/3.6	0.008/10.8	0.0064/19.5	0.014/42.3	1.24/ 50	0.16/150	0.104/142.6
4 shorted turns and 2 bars	0.166/4.2	0.044/12.6	0.006/21.0	0.02/41.7	0.98/ 50	0.14/150	0.046/141.6
15 shorted turns and 2 bars	0.202/4.2	0.046/12.6	0.0042/21.0	0.026/41.7	0.68/ 50	0.02/150	0.046/141.6
25 shorted turns and 2 bars	0.224/4.2	0.046/12.6	0.0072/21.0	0.018/41.7	0.56/50	0.12/150	0.054/141.6

Type of damage	f_0	$3f_0$	$3f_0+[n_s(1-s)\,m]/60$			
			$m=2$	$m=-1$	$m=-2$	$m=-3$
4 shorted turns and 2 bars	1/ 50	0.013/ 150	0.0108/195.8	0.0012/127.1	0.0106/104.2	0.00112/81.3
15 shorted turns and 2 bars	0.66/ 50	0.022/ 150	0.020/195.8	0.0012/127.1	0.0126/104.5	0.00024/81.3
25 shorted turns and 2 bars	0.54/ 50	0.06/ 150	0.022/195.8	0.0024/127.1	0.0114/104.5	0.02/ 81.3
4 shorted turns	1.10/ 50	0.012/ 150	0.00074/196.2	0/252.2	0/207.4	0.0004/80.7
15 shorted turns	0.76 /50	0.026/ 150	0.00144/196.2	0.0010/126.1	0/207.4	0.00030/80.7
25 shorted turns	0.42/ 50	0.048/ 150	0.0024/ 196.2	0.0004/126.1	0.0004/103.8	0.0004/80.7

For: $R = 21.5\ \Omega$, 4 shorted turns – 0.1 A, 15 shorted turns – 0.3 A, 25 shorted turns – 0.65 A

According to the presented measurements and calculation results from Fig. 7 and 8, the occurrence of slight inter-turn short circuits in the stator phase produces a growth in the amplitude of the third supply harmonic, while at the same moment, a weakness of the flux of the supply frequency can be observed. Upon a combined damage to rotor and stator circuits, an interaction of the rotor and the stator magnetic fields can be observed, expressed by the occurrence of sums and differences of the components as described (5) and equal to twice the slip fundamental frequency (2). The basic feature of the combined damage to rotor and stator circuits is the lack of significant differences in the amplitudes of the components associated with the asymmetry of the rotor (1), (3) and (4) relative to an induction motor with the rotor circuit damage only.

4.2. Non-stationary analysis

The operating states of an induction motor in transient conditions [7, 8] can be divided into electrodynamic and electromechanical transient states. In the first case, the waveforms of electromagnetic and mechanical quantities vary with comparable speed. In the above operating condition, extraction of the diagnostic signal (which is an electrodynamic quantity) from the total current waveform is considerably more difficult or even impossible.

Therefore, the most often considered transient state in the diagnostics of induction motors is an electromagnetic transient state, where it is assumed that the electromagnetic quantities change as a function of time at a constant speed. In this case, the preferred option is a long duration of the electromagnetic transient state, a typical example of this is the heavy start-up of an induction motor.

As shown in [9, 11], also in the case of the voltage waveform proportional to the axial flux in the transient state and the dynamic state, similarly as in the analysis of the stator current, the low-frequency methods can be applied successfully in the comparative analysis of diagnostics signals' fluctuation. As it will be proven later in the article, a precise observation of changes in selected diagnostic signals is only possible when using the time-frequency methods.

Below, one can find some examples of spectrograms made with the use of the short-time Fourier transform [15, 20] during the start-up of the symmetrical motor and the motor with one damaged bar of the cage. The below examples were selected for the induction motors operating in steady states and loaded at 7 amps stator currents. In the analysis, a short-time Hanning window with a duration of 0.2 seconds was applied. The frequency band under observation was limited to the frequency range 0–150 Hz, where the amplitudes of diagnostic signals associated with the rotor circuit achieved the greatest values. The obtained spectrograms were supplemented by the theoretical waveform of the diagnostic signals during the start-up (Fig. 9).

According to the spectrograms presented in Figs. 10 and 11, a common feature is the presence of the supply fundamental component and primary slip frequency (2). For an induction motor with one damaged cage bar, one can observe the change in time of the components described by formulas (1) – [for $k = 3,5,7$] and (3) – [for $k = 3$]. Despite the short time of the motor start, the basic diagnostic signals remain clearly visible, which does not happen in the case of the stator current analysis, where it is required that the starting time of the induction motor is at least 1.5s.

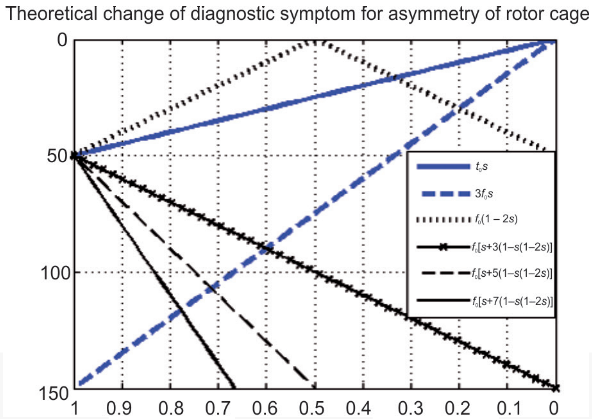

Fig. 9. Theoretical change of diagnostic symptoms for the asymmetry of the rotor cage for different motor loads

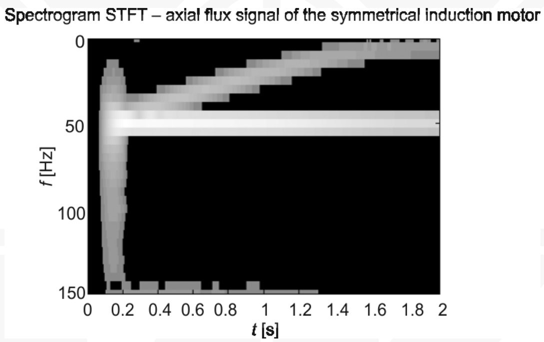

Fig. 10. Spectrogram STFT – axial flux signal of the symmetrical induction motor

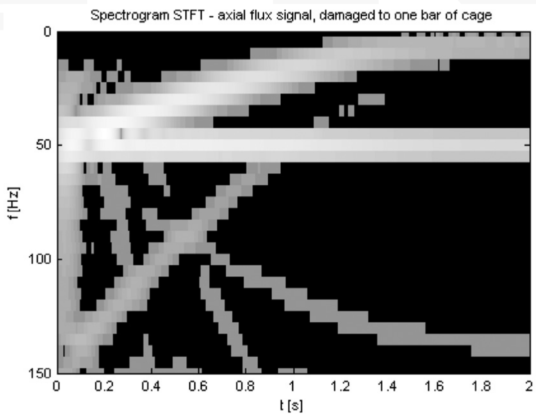

Fig. 11. Spectrogram STFT – axial flux signal, one damaged bar of the cage

Fig. 12 presents the course of observed diagnostic signals in the time domain for the frequency of 125 Hz. The observed frequency was selected in view of the possibility to observe all relevant diagnostic signals associated with the cage rotor circuit, with the exception of the signal (2). The frequency band in the range of 100–150 Hz should be considered universal to evaluate the technical condition of the cage rotor during the start-up because the pattern of the diagnostic signals remains constant regardless of the design parameters of the induction motor.

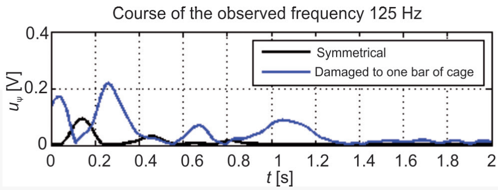

Fig. 12. Change of the observed frequency 125 Hz

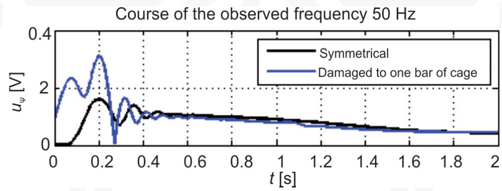

Fig. 13. Course of the observed frequency 125 Hz

5. Conclusions

Among the most important advantages of using the signal of the axial flux as a diagnostic signal, one should point the lack of significant influence of such physical quantities as the torque and supply frequency on the readability of the spectrum.

As it was shown, the greatest benefit from the axial flow analysis can be obtained in the initial stage of development of any asymmetry of electrical origin in the form of damage to the rotor and the stator. In addition, the analysis of the flux axial signal requires less effort than the calculations for the purposes of the stator current analysis.

One of the disadvantages of using the axial flux as a diagnostic signal seems to be the lack of measurement of the operational quantities in the form of voltage or current as well as the need to use measuring coils of different diameters customized to the mechanical size of the induction motor, in the case of the coil location inside or outside the bearing shield.

In the future research concerning the use of the axial flux, the authors plan to create a database of measurements for high-power induction motors and the detailed elaboration of the statistical data for different duties and mechanical loads – this is required to develop a reliable indicator of technical condition of a wide range of power of induction motors.

Acknowledgment

Presented results of the research, which was carried out under the theme No. E-2/581/2016/DS, were funded by the subsidies on science granted by Polish Ministry of Science and Higher Education.

References

[1] Biernat A., Góralski P., *Zastosowanie pomiaru strumienia osiowego do okresowej diagnostyki silników indukcyjnych w zakładach przemysłowych*, Zeszyty Problemowe – Maszyny Elektryczne nr 4/2014 (104), wyd. BOBRME Komel, 247–252.

[2] Duda A., Petryna J., Sułowicz M., Guziec K., *Metoda wstępnej oceny stanu wirnika silnika indukcyjnego przy pomocy dedykowanego przyrządu opartego na pomiarze strumienia poosiowego*, Zeszyty Problemowe – Maszyny Elektryczne nr 2/2015 (106), wyd. BOBRME Komel, 59–63.

[3] Frosini L., Borin A., Girometta L., Venchi G., *A novel approach to detect short circuits in low voltage induction motor by stray flux measurement*, Electrical Machines (ICEM), 2012 XXth International Conference on Marseille.

[4] Glinka T., *Maszyny elektryczne i transformatory. Podstawy teoretyczne, eksploatacja i diagnostyka*, Instytut Napędów i Maszyn Elektrycznych KOMEL 2015.

[5] Gołębiowski L., Gołębiowski M., Noga M., Skwarczyński J., *Strumień osiowy w modelu 3D MES maszyny indukcyjnej*, Elektrotechnika i Elektronika, Tom 25, Zeszyt 2, 2006.

[6] Kokko V., *Condition Monitoring of Squirrel-Cage Motors by Axial Magnetic Flux Measurements*, Department of Electrical Engineering, Optoelectronics and Measurement Techniques Laboratory, University of Oulu, Oulu 2003.

[7] Kowalski Cz.T., *Diagnostyka układów napędowych z silnikiem indukcyjnym z zastosowaniem metod sztucznej inteligencji*, Oficyna Wydawnicza Politechniki Wrocławskiej, Wrocław 2013.

[8] Paszek W., *Stany nieustalone maszyn elektrycznych prądu przemiennego*, WNT, Warszawa 1986.

[9] Petryna J., Sułowicz M., Duda A., *Wykorzystanie strumienia poosiowego do badania stanów dynamicznych maszyn indukcyjnych małej i dużej mocy*, Zeszyty Problemowe – Maszyny Elektryczne nr 2/2014 (102), wyd. BOBRME Komel, 165–171.

[10] Petryna J., Sułowicz M., Puzio Ł., Dziechciarz A., *Wykrywanie zwarć zwojowych w maszynach elektrycznych na stacji prób z wykorzystaniem cewki do pomiaru strumienia poosiowego*, Zeszyty Problemowe – Maszyny Elektryczne nr 2/2015 (106), wyd. BOBRME Komel, 185–190.

[11] Petryna J., Sułowicz M., Duda A., Guziec K., *Wykorzystanie strumienia unipolarnego w diagnostyce maszyn prądu przemiennego*, Zeszyty Problemowe – Maszyny Elektryczne nr 2/2013 (99), wyd. BOBRME Komel, 85–90.

[12] Pietrowski W., *Zastosowanie radialnej sieci neuronowej w diagnostyce uszkodzeń uzwojenia stojana maszyny indukcyjnej klatkowej*, Zeszyty Problemowe – Maszyny Elektryczne nr 88/2012, wyd. BOBRME Komel, 93–96.

[13] Pole G.O., *Application of Magnetic Fields To Aid The Detection and Diagnosis of Induction Motor Drive Faults*, University of Wales Institute Cardiff, January 2009.

[14] Pusca R., Romary R., Fireteanu V., Ceban A., *Finite Element Analysis and Experimental Study of The Near-Magnetic Field for Detection of Rotor Faults in Induction Motors*, Progress in Electromagnetics Research B, Vol. 50, 2013, 37–59.

[15] Swędrowski L., *Pomiary w diagnostyce silników indukcyjnych klatkowych*, Wydawnictwo Politechniki Gdańskiej, Gdańsk 2013.

[16] Szymaniec S., *Badania, eksploatacja i diagnostyka zespołów maszynowych z silnikami indukcyjnymi*, Oficyna Wydawnicza Politechniki Opolskiej, Opole 2013.

[17] Tulicki J., Sułowicz M., *Zastosowanie strumienia poosiowego do oceny stanu technicznego silnika klatkowego w trakcie rozruchu. Część I: Niesymetria wirnika*, Zeszyty Problemowe – Maszyny Elektryczne nr 2/2016 (110), wyd. BOBRME Komel, 147–154.

[18] Tulicki J., Sułowicz M., *Zastosowanie strumienia poosiowego do oceny stanu technicznego silnika klatkowego w trakcie rozruchu. Część II: Zwarcia zwojowe, łączna asymetria obwodu stojana i wirnika*, Zeszyty Problemowe – Maszyny Elektryczne nr 2/2016 (110), wyd. BOBRME Komel, 155–162.

[19] Weinreb K., Duda A., Petryna J., Sułowicz M., *Diagnostyka ekscentryczności silnika indukcyjnego w oparciu o pomiar strumienia poosiowego*, Zeszyty Problemowe – Maszyny Elektryczne nr 2/2015 (106), wyd. BOBRME Komel, 13–20.

[20] Zieliński T.J., *Cyfrowe przetwarzanie sygnałów. Od teorii do zastosowań*, Wydawnictwa Komunikacji i Łączności, 2007.

[21] Pietrowski W., *Wavelet analysis of axial flux in an induction machine on no-load test*, Przegląd Elektrotechniczny, Vol, 7b, 2012, 20–23.

[22] Pietrowski W., *Application of Radial Basis Neural Network to diagnostics of induction motor stator faults using axial flux*, Przegląd Elektrotechniczny, Vol. 6, 2011, 190–192.

[23] Głowacz A., *Diagnostics of direct current machine based on analysis of acoustic signals with the use of symlet wavelet transform and modified classifier based on words*, Eksploatacja i Niezawodność – Maintenance and Reliability, Vol. 16, no. 4, 2014, 554–558.

[24] Ludwinek K., *Measurement of momentary currents by Hall linear sensor*, Przegląd Elektrotechniczny, Vol. 85, Issue 10, 2009, 182–187.

[25] Głowacz A., Głowacz Z., *Diagnostics of induction motor based on analysis of acoustic signals with application of FFT and classifier based on words*. Archives of Metallurgy and Materialsvol, 55, issue. 3, 2010, 707–712.